1521-009X/12/4001-169–177$25.00
DRUG METABOLISM AND DISPOSITION
Vol. 40, No. 1
41137/3740016
Copyright © 2012 by The American Society for Pharmacology and Experimental Therapeutics
DMD 40:169–177, 2012

DRUG METABOLISM & DISPOSITION

Acetaminophen-Induced Hepatotoxicity in a Liver Tissue Model Consisting of Primary Hepatocytes Assembling around an Endothelial Cell Network

Yu Toyoda, Miho Tamai, Kasumi Kashikura, Shunsuke Kobayashi, Yoichi Fujiyama, Tomoyoshi Soga, and Yoh-ichi Tagawa

Department of Biomolecular Engineering, Graduate School of Bioscience and Biotechnology, Tokyo Institute of Technology, Yokohama, Japan (Y.To., M.T., S.K., Y.Ta.); Institute for Advanced Biosciences Keio University, Yamagata, Japan (K.K., T.S.); and Optical Components Consumer & Optical Products Department Shimadzu, Corporation, Kyoto, Japan (Y.F.)

Received June 10, 2011; accepted October 18, 2011

ABSTRACT:

Primary hepatocytes have been used in drug development for the evaluation of hepatotoxicity of candidate compounds. However, the rapid depression of their hepatic characters in vitro must be improved to predict toxicity with higher accuracy. We have hypothesized that a well organized tissue construct that includes nonparenchymal cells and appropriate scaffold material(s) could overcome this difficulty by remediating the viability and physiological function of primary hepatocytes. In this study, we constructed an in vitro liver tissue model, consisting of mouse primary hepatocytes assembling around an endothelial cell network on Engelbreth-Holm-Swarm gel, and examined its response to acetaminophen treatment. The increase in lactate dehydrogenase release after the exposure to acetaminophen was induced earlier in the liver tissue model than in monolayer hepatocytes alone, suggesting that the tissue model was more sensitive to an acetaminophen-induced toxicity. On the basis of our results, we conclude that liver tissue models of this kind may enhance the responses of hepatocytes against xenobiotics via the maintenance of hepatic genes and functions such as cytochrome P450s. These findings will contribute to the development of more accurate systems for evaluating hepatotoxicity.

Introduction

Despite the dramatic and evolutional progress made in life sciences over the last decade, the productivity of pharmaceutical companies in bringing new drugs to the market has not been improved (Kola and Landis, 2004; Paul et al., 2010). Nonetheless, research and development expenditure has been increasing, and the high rate of candidate attrition during development has been a considerable problem. To address these issues, a great deal of effort has been devoted toward reducing the candidate attrition in the late stages of drug development, as well as toward producing new drugs more cost effectively (Gleeson et al., 2011; Kwong et al., 2011). It is important to predict and/or detect the toxicity of the drug candidates as early as possible during the process of drug development.

The liver is a multifunctional organ involved in the metabolism, detoxification, and excretion of substances. Therefore, compound-induced hepatotoxicity is a major issue in drug discovery and development (Jaeschke et al., 2002; Kaplowitz, 2005). Although many in vitro trials have used primary cultured hepatocytes prepared from the liver, these cells pose several problems for in vitro hepatotoxicity assays. When cultured by themselves, hepatocytes cannot continue to grow or maintain their specific functions in vitro. The liver is composed of not only parenchymal hepatocytes but also nonparenchymal cells, such as sinusoidal endothelial cells, Kupffer cells, and others. Hepatocytes can express their specific functions only in the structural environment of hepatic tissue. To make it possible for primary hepatocytes to survive for long periods and maintain their specific functions in vitro, it is important to maintain cell-cell interactions, both between hepatocytes and between hepatocytes and nonparenchymal cells (Bhatia et al., 1998, 1999; Strain, 1999; Kidambi et al., 2009), as

This work was supported by the Precursory Research for Embryonic Science and Technology and the Adaptable and Seamless Technology transfer Program through target-driven R&D funding [Grant AS2211513G] from the Japan Science and Technology Agency (JST); a Grant-in-Aid for Scientific Research (B) [Grant 21300178] from the Japanese Society for the Promotion of Science (JSPS); and a Grant-in-Aid for Scientific Research on Innovative Areas [Grant 23119003] from the Ministry of Education, Culture, Sports, Science and Technology. Y.To. and M.T. are JSPS research fellows.

Article, publication date, and citation information can be found at http://dmd.aspetjournals.org.

http://dx.doi.org/10.1124/dmd.111.041137.

ABBREVIATIONS: ECM, extracellular matrix; ES, embryonic stem; IVL^{mES}, mouse ES cell-derived in vitro liver tissue model; HUVEC, human umbilical vein endothelial cell; NAPQI, *N*-acetyl-*p*-benzoquinone imine; IVL, in vitro liver model; APAP, *N*-(4-hydroxyphenyl)acetamide; EHS, Engelbreth-Holm-Swarm; OHT, hydroxytestosterone; HP, hydroxyprogesterone; EGM-2, endothelial cell growth medium-2; DMEM, Dulbecco's modified Eagle's medium; HBSS, Hank's balanced salt solution; LDH, lactate dehydrogenase; HPLC, high-performance liquid chromatography; CE-TOFMS, capillary electrophoresis coupled with electrospray ionization time-of-flight mass spectrometry; PECAM-1, platelet endothelial cell adhesion molecule-1; vWF, Von Willebrand factor; HGF, hepatocyte growth factor; IVL_{EHS}, in vitro liver model on EHS gel; RT-PCR, reverse transcription-polymerase chain reaction; hprt, hypoxanthine-guanine phosphoribosyltransferase; TAT, tyrosine aminotransferase.

Downloaded from dmd.aspetjournals.org at ASPET Journals on July 19, 2018

well as proper extracellular matrix (ECM) (Kleinman et al., 2003; Takashi et al., 2007).

In this context, we have focused on the interaction between hepatocytes and endothelial cells. In 2005, we successfully achieved hepatic organogenesis from murine embryonic stem (ES) cells (Ogawa et al., 2005; Tsutui et al., 2006). This mouse ES cell-derived in vitro liver tissue model (IVL^{mES}) included both hepatocyte layers and a sinusoid vascular network; the model was capable of recapitulating most hepatic functions. Due to imperfect control of the hepatic regions in IVL^{mES}, it was difficult to quantitatively evaluate metabolites in this system. However, Nahmias et al. (2006) reported a culture system, "liver-like tissue" that included fewer components. Their system consists of two types of cells, primary hepatocytes and an endothelial cell network that formed vascular structures. As with IVL^{mES}, liver-like tissue exhibited long-term expression of hepatic genes such as albumin. It would be reasonable to expect that an optimized liver-like tissue would be a useful system for evaluating the hepatotoxic potential of candidate drug compounds.

In this study, we used both mouse primary hepatocytes and human umbilical vein endothelial cells (HUVECs), a representative type of endothelial cells, to construct an in vitro liver model (IVL) for use in drug screening. Using these two types of cells allowed us to specifically examine the expression of hepatic genes and resulted in development of a simple, cost-effective system. Next, we investigated the response of IVL to xenobiotic treatment to assess the utility of this system in the evaluation of hepatotoxicity.

Acetaminophen [APAP; *N*-(4-hydroxyphenyl)acetamide; $C_8H_9NO_2$] is one of the most commonly used drugs for the treatment of pain and fever; its reactive metabolite, *N*-acetyl-*p*-benzoquinone imine (NAPQI), oxidized by cytochrome P450 isozymes such as CYP2E1, causes hepatocyte damage (Hayes and Pickering, 1985; Lee et al., 1996; Jaeschke et al., 2003; James et al., 2003). Compared with an in vivo acute liver injury model, in vitro trials using monolayer-cultured hepatocytes generally requires more time for the definite observation APAP cytotoxicity. We have hypothesized that the gap between in vivo and in vitro hepatic reactions could be filled using a well organized tissue construct that included nonparenchymal cells and appropriate scaffold matrix to improve the viability and physiological function of hepatocytes.

To verify this hypothesis, we have constructed an in vitro liver tissue model and examined its response to APAP treatment. In short-term culture, our liver tissue model was more sensitive to APAP-induced toxicity than were hepatocytes alone. Our results suggest that the presence of endothelial cells enhances the responsiveness of hepatocytes to xenobiotics.

Materials and Methods

Cells and Materials. HUVECs were obtained from Cambrex BioScience Walkersville, Inc. (Walkersville, MD). EBM-2 (endothelial cell basal medium) and EGM-2 Single Quots (supplemental factors) were purchased from Lonza Japan Ltd. (Tokyo, Japan). Dulbecco's modified Eagle's medium (DMEM), penicillin/streptomycin (100×), and trypsin-EDTA were from Invitrogen (Carlsbad, CA). Tissue-culture treated cell culture dishes/plates were acquired from Corning Inc. (Tokyo, Japan). Collagenase, trypsin inhibitor, mannitol, D-camphor-10-sulfonic acid, 1,3,5-benzenetricarboxylic acid (trimesate) and gelatin were purchased from Wako Pure Chemical Industries, Ltd. (Osaka, Japan). 2-(*N*-morpholino)ethanesulfonic acid was obtained from Dojindo Laboratories (Kumamoto, Japan). Laminin, fibronectin, poly-D-lysine, collagen type I, collagen type IV, and growth factor-reduced Engelbreth-Holm-Swarm (EHS) gel were purchased from BD Biosciences (Bedford, MA), and stored at −30°C until use. Acetaminophen (*p*-acetamidophenol) was purchased from Nacalai Tesque, Inc. (Kyoto, Japan). Testosterone (4-androsten-17β-ol-3-one), 6β-hydroxytestosterone (OHT), 2α-OHT, and 11α-hydroxyprogesterone (HP) were purchased from Sigma-Aldrich (St. Louis, MO). 16α-OHT, 16β-OHT, and 7α-OHT were purchased from Daiichi Pure Chemicals Corp. (Tokyo, Japan). 3-(*N*-acetyl-L-cysteine-*S*-yl)acetaminophen (acetaminophen mercapturate) was obtained from Santa Cruz Biotechnology, Inc. (Santa Cruz, CA). All reagents used were of analytical grade.

Animals. Male, 6- to 10-week-old BALB/cAJc1 mice were purchased from CLEA Japan Inc. (Tokyo, Japan) and were treated in accordance with local institutional guidelines for the care and use of laboratory animals. DsRed2 transgenic mice carrying the expression vector of DsRed2 fluorescence protein gene, controlled by the CAG promoter, were originally obtained via a DsRed2-expressing ES cell-contributing chimera mouse produced by the aggregation chimera method. The F_1 offspring expressing DsRed2 protein has been backcrossed with BALB/cAJcl mice finally to 20 generations. DsRed2 BALB/cAJcl transgenic mice (male, 6-week-old) were used in this study for DsRed2 fluorescent assay. The animal protocol was approved by the Animal Experimentation Committees of Tokyo Institute of Technology.

Preparation of Cell Culture Substrate. Gelatin-coated surfaces were prepared by incubation with heat-sterilized 0.05% gelatin solution for 3 h at 4°C. Thawing EHS gel was poured into ice-cold 6-well plates (500 μl/wells) and incubated for 30 min at 37°C to allow polymerization. Laminin, fibronectin, poly-D-lysine, collagen type I, and collagen type IV (50 μg protein/well) were coated onto surfaces according to the manufacturer's instructions.

Cell Culture. HUVECs were maintained in complete EGM-2 [EBM-2 with instructed supplementations as follows: 2% (v/v) fetal bovine serum, hydrocortisone, human fibroblast growth factor-β, vascular endothelial growth factor, R3-IGF-1, ascorbic acid, human epidermal growth factor, GA-1000 (Gentamicin, Amphotericin-B), and heparin] at 37°C in a humidified atmosphere of 5% CO_2 in air. The passage of cells was limited to 10 times. Isolated hepatocytes were maintained in DMEM supplemented with 100 U/ml penicillin and 100 μg/ml streptomycin at 37°C in a humidified atmosphere of 5% CO_2 in air.

Isolation of Primary Hepatocytes from Mouse Liver. Hepatocytes were prepared from mice anesthetized with pentobarbital by an in situ 2-step collagenase perfusion method (Seglen, 1976), with slight modifications. In brief, after the cannulation of isolated portal vein with a 24-gauge catheter (Terumo, Tokyo, Japan), mouse liver was preperfused in situ with Hank's balanced salt solution (HBSS) containing EGTA (0.19 g/l) and glucose (0.98 g/l) to remove the blood; next, the liver was perfused with 0.015% collagenase in HBSS. After the extraction of the liver, the cells were dispersed in ice-cold HBSS (pH 7.2) by blade mincing. The cells obtained were filtered through a 100-μm pore mesh nylon cell strainer (BD Biosciences) and centrifuged twice for 2 min at 500*g* to remove nonparenchymal cells. Subsequently, for further purification, the remaining cells were centrifuged for 2 min at 1200*g* and then subjected to 40% Percoll density gradient centrifugation for 10 min at 1200*g*. At this stage, cell viability measured by the trypan blue method was >85%. The isolated hepatocytes were plated at a cell density of 1.0×10^6 cells per well in 6-well plates; cells were grown in DMEM containing 10% (v/v) heat-inactivated fetal bovine serum, 100 U/ml penicillin, and 100 μg/ml streptomycin at 37°C in a humidified incubator with 5% CO_2/95% air. The medium for cell attachment was replaced with fresh medium after the first 4 h of incubation. One day later, the growth medium was exchanged with serum-free medium, and replaced daily thereafter.

Detection of mRNA by Reverse Transcription-Polymerase Chain Reaction. Total RNA was isolated using the acid guanidinium-phenol-chloroform method according to a standard protocol described elsewhere. The purity and concentrations of isolated RNA were assessed by absorbance determination, and the integrity of the RNA was verified by 0.6% agarose gel electrophoresis in TAE buffer (20 mM Tris acetate, 0.5 mM EDTA, pH 8.0). First-strand cDNA was prepared from the extracted total RNA in a reverse-transcriptase reaction, using the SuperScript II Reverse Transcriptase kit and oligo(dT) primer (Invitrogen) according to the manufacturer's instruction. The cDNA from mRNA of the genes of interest were amplified by PCR in a GeneAmp PCR System 9700 thermal cycler (Applied Biosystems, Foster City, CA) with a set of specific primers (Tables 1 and 2). After the PCR, the resulting amplicons were separated by 1.5% (w/v) agarose gel electrophoresis with TBE buffer (44.5 mM Tris, 44.5 mM boric acid, 10 mM EDTA, pH 8.0) and detected with ethidium bromide under UV light.

Urea Assay. Culture medium collected in each measurement period was centrifuged for 5 min at 300*g* to remove floating cells, and supernatant was

Downloaded from dmd.aspetjournals.org at ASPET Journals on July 19, 2018

TABLE 1

Primer information for human gene

Gene	GenBank Accession Number	Sequences (5′>3′)	Position	Product
				bp
PECAM1	NM_000442	F: ACGGAATCCTTCTCTACACC	901–920	477
		R: TGCAGTGCAGATATACGTCC	1377–1358	
vWF	NM_000552	F: TGCAACACTTGTGTCTGTCG	2786–2805	486
		R: TGCAGTGCAGATATACGTCC	3271–3251	
HGF	NM_000601	F: CCGAACAGGATTCTTTCACC	101–120	372
		R: TATTGAAGGGGAACCAGAGG	472–453	
GAPDH	NM_002046	F: AGATCATCAGCAATGCCTCC	536–555	492
		R: TGACAAAGTGGTCGTTGAGG	1027–1008	

F, forward; r, reverse; bp, base pairs.

stored at −80°C until determination of urea levels. Urea was detected in culture medium using a QuantiChrom Urea Assay Kit (BioAssay Systems, Hayward, CA). In brief, 5 μl of the obtained solvent was incubated with a 200-μl reaction mixture for 30 min at room temperature. The urea-dependent chromogenic reaction was read using an iMark Microplate Reader (Bio-Rad Laboratories, Hercules, CA) at 492 nm. To calculate the urea concentration of each sample, known concentrations of urea were used to generate a standard curve.

WST-1 Assay. The viability of cells was evaluated using a Cell Counting Kit (Dojindo Laboratories). In brief, cells were seeded in 96-well plates (4×10^4 cells/well) and cultured at 37°C for 24 h. Acetaminophen was added to the culture medium at various concentrations, and incubation was continued for an additional 24 h. Subsequently, the culture medium was replaced with 110 μl of fresh medium containing 10% (v/v) of the WST-1 assay reaction mixture. Cells were again incubated for 90 min, and 100 μl of the resulting supernatant was transferred to a 96-well microplate. The reduction of WST-1 was measured photometrically using an iMark Microplate Reader at 450 nm.

Lactate Dehydrogenase Assay. After incubation for the indicated periods, the culture medium was collected and centrifuged for 5 min at 300*g*, and the supernatant was used for determination of lactate dehydrogenase (LDH) level in the culture medium. To detect the LDH levels in whole-cell lysate, the remaining cells were treated with 10 mM phosphate buffer (pH.7.4) containing 1% (w/v) Triton X-100. The cell suspension sample containing the dissolved scaffold materials was homogenized by passage through a 27-gauge needle and then centrifuged for 10 min at 800*g* at 4°C. The resulting supernatant fraction (whole-cell lysate) was transferred to a new tube. LDH levels in each fraction (culture medium and whole-cell lysate) were detected using SPOTCHEM EZ SP-4430 and SPOTCHEM II LDH (ARKRAY, Kyoto, Japan). Media-released LDH ratio (percentage) was calculated using the following formula: media-released LDH ratio (%) = $LDH_{media}/(LDH_{media} + LDH_{whole\text{-}cell\ lysate}) \times 100$.

Fluorescence Intensity Assay. To count the amount of living hepatocytes quantitatively, DsRed2 fluorescence intensity was measured 24 h after the seeding of red hepatocytes isolated from the DsRed-transgenic mouse. The DsRed2 fluorescence derived from the living red-fluorescent hepatocytes attaching on the culture surface was measured by using LAS-4000 system (Fujifilm, Tokyo, Japan). Obtained images were analyzed by Multi Gauge program, version 3.1 (Fujifilm).

Testosterone Metabolism Assay. To examine the enzymatic activities of cytochrome P450s, each metabolite of testosterone in the culture medium was quantitatively detected using high-performance liquid chromatography (HPLC) as described previously (Tsutui et al., 2006) with some modification. In brief, testosterone and its metabolites were separated using an HPLC system (LC-10AD VP; Shimadzu, Kyoto, Japan) equipped with a reversed-phase C18 column (Cadenza CD-C18, 10 mm × 250 mm; Tosoh, Tokyo, Japan) maintained at 40°C. Elution solvents were as follows: solvent A (water/methanol/acetonitrile: 39:60:1 v/v) and solvent B (water/methanol/acetonitrile: 80:18:2 v/v). Elution was started with 18% solvent B and 82% solvent A for 10 min, followed by elution with a linear gradient of solvent B (18–80%) for the next 10 min. Afterward, 80% solvent B was maintained for 30 min. The elution flow throughout was kept constant at a rate of 0.5 ml/min, and testosterones were detected by UV absorbance at 254 nm. The resulting chromatograms were analyzed using the LC Solutions software (Shimadzu). The peak of each metabolite was compared with that of the internal standard to determine its quantity. To obtain the standard chromatogram, 2α-OHT, 6β-OHT, 7α-OHT, 11α-HP, 16α-OHT, and 16β-OHT were subjected to independent analyses.

CE-TOFMS Analysis. 3-(*N*-acetyl-L-cysteine-*S*-yl)acetaminophen, one of the APAP metabolites, was detected using the CE-TOFMS method as described previously (Soga et al., 2006). In brief, after the 5% mannitol treatment, cells on the EHS gel were saturated with 1 ml of MeOH containing 25 μM of each internal standard (methionine sulfate, 2-(*N*-morpholino)ethanesul-

TABLE 2

Primer information for mouse gene

Gene	GenBank Accession Number	Sequences (5′>3′)	Position	Product
				bp
Albumin	NM_009654	F: GCTACGGCACAGTGCTTG	1224–1241	266
		R: CAGGATTGCAGACAGATAGTC	1489–1469	
Tat	NM_146214	F: CAATCCTGGACAGAACATCC	565–584	280
		R: GATCTCATCGGCTAAGATGG	844–825	
Cyp1a2	NM_009993	F: GTCACCTCAGGGAATGCAGTGG	744–765	493
		R: AGGTGTCCCTCGTTGTGCTGTG	1236–1215	
Cyp2e1	NM_021282	F: TGTGACTTTGGCCGACCTGTTC	889–910	446
		R: CAACACACACGCGCTTTCCTGC	1334–1313	
Cyp2r1	NM_000442	F: CGGAAGATGCAGTTGTACGTGGC	1166–1188	477
		R: TCTGCACAGATGAGGTAGGGCTG	1511–1489	
Cyp3a	NM_007818	F: AATTCCTGGGCCCAAACCTCTGC	189–211	496
		R: AGGATCCTCTGGGTTGTTGAGGG	684–662	
Abcb11	NM_021022	F: TGGCCAGATCACCAACGAAGCC	2935–2956	513
		R: TGCCCAGGATCCACAGATACCG	3447–3426	
Abcc2	NM_013806	F: TGTGGATAATGAGGCGCCGTGG	3921–3942	452
		R: TGGAGCAACCCAAGTTGCAGGC	4373–4352	
Hprt	NM_013556	F: GTAATGATCAGTCAACGGGG	463–482	441
		R: AGCTTTACTAGGCAGATGGC	903–884	

F, forward; r, reverse; bp, base pairs.

Downloaded from dmd.aspetjournals.org at ASPET Journals on July 19, 2018

fonic acid, and D-camphor-10-sulfonic acid) for 10 min to extract the metabolites. The resulting solution was immediately mixed with 400 μl of $CHCl_3$ and 200 μl of water and centrifuged at 10,000*g* for 3 min at 4°C. Subsequently, the 400-μl upper aqueous layer was centrifugally filtered through a Millipore 5-kDa cutoff filter (Millipore Corporation, Billerica, MA) to remove proteins. The filtrate was lyophilized and dissolved in 50 μl of MilliQ water containing reference compounds (3-aminopyrrolidine and trimesate) before CE-TOFMS analysis.

CE-TOFMS analysis was performed using an Agilent CE capillary electrophoresis system (Agilent Technologies, Waldbronn, Germany), an Agilent G3250AA LC/MSD TOF system (Agilent Technologies, Palo Alto, CA), an Agilent1100 series binary HPLC pump, a G1603A Agilent CE-MS adapter, and a G1607A Agilent CE-ESI-MS sprayer kit. For system control and data acquisition, we used the G2201AA Agilent ChemStation software for CE and the Analyst QS software for TOFMS. CE-TOFMS analysis for anionic metabolites was carried out according to a previous report (Soga et al., 2009).

Statistical Tests. Experimental data were expressed as means ± S.D. and analyzed by determining the statistical significance according to Student's *t* test. Differences were considered significant when $P < 0.05$.

Results

Establishment and Characterization of the In Vitro Liver Tissue Model on EHS Gel. HUVECs, a representative type of endothelial cells, were seeded on several scaffold materials (gelatin, laminin, fibronectin, poly-D-lysine, collagen type I, collagen type IV, or EHS gel), to investigate what kind of scaffold material is useful for inducing the functions of endothelial cell. As shown in Fig. 1A, HUVECs grew with normal spreading and displayed a cobblestone morphology within 24 h when grown on laminin, fibronectin, poly-D-lysine, collagen type I, or collagen type IV, as well as on gelatin-coated or noncoated tissue culture 6-well plates. However, on EHS gel, HUVECs rapidly elongated and generated a network structure (Fig. 1A). After the seeding of HUVECs (3.5×10^5 cell/well in 6-well plates), network morphogenesis on EHS gel was accomplished within a few hours and could be maintained for at least 4 days (Fig. 1B). Subsequently, to compare the maintenance of endothelial cell character of HUVECs on each scaffold material, we measured the expression of endothelial cell-specific marker genes, such as *platelet endothelial cell adhesion molecule-1* (*PECAM-1*) and *Von Willebrand factor* (*vWF*) (Fig. 1C). In HUVECs cultured on EHS gel, expression of these genes was maintained at a high level compared with cells grown on other scaffold materials. It is noteworthy that hepatocyte growth factor (HGF) was strongly expressed in HUVECs only on EHS gel (Fig. 1C).

On this network structure of HUVECs, freshly isolated mouse primary hepatocytes (1.0×10^6 cell/well in 6-well plates) were seeded and cultured. The primary hepatocytes migrated toward the HUVEC network and piled next to one another within 24 h, forming a structure that resembled hepatic tissue (Fig. 1, D and E). This structure could be maintained for 5 days, at least until the disruption of HUVEC network. In the absence of a HUVEC network, primary hepatocytes seeded on EHS gel almost never aggregated with each other. The presence of HUVEC on gelatin did not affect the cobblestone morphology of hepatocytes (Fig. 1D). According to the scheme described in Fig. 1F, this in vitro liver tissue model on EHS gel, which we term IVL_{EHS}, was used in the following experiments.

To confirm whether there was no difference in the percentage of attachment of hepatocytes between gelatin and EHS gel, we used red-fluorescent hepatocytes from the livers of DsRed2-transgenic mice. Based on the linear relationship between the signal intensity of DsRed2 fluorescence and the total amount of red hepatocytes (Fig. 1G), the number of hepatocytes finally attaching on the surface of each culture conditions was almost the same (Fig. 1H).

The IVL_{EHS} Could Maintain Its Hepatic Function for a Longer Period than Monolayer Culture of Hepatocytes. To compare the effect of the IVL_{EHS} to general primary hepatocyte culture on gelatin, we investigated the level of urea production, a major hepatic function (Fig. 2). After the first 24 h, urea production did not differ between samples, regardless of whether primary hepatocytes were cocultured with HUVECs or whether they were grown on gelatin or EHS gel; however, urea levels in the culture were lower when the cells were grown on EHS gel than on gelatin (Fig. 2A). The urea level in the culture medium of the HUVEC network alone was too low (less than several hundred micrograms per deciliter) to recognize a significant effect (data not shown). To estimate the ratio of decrease in relative urea levels on EHS gel (Fig. 2A), identical volumes (2.0 ml) of urea

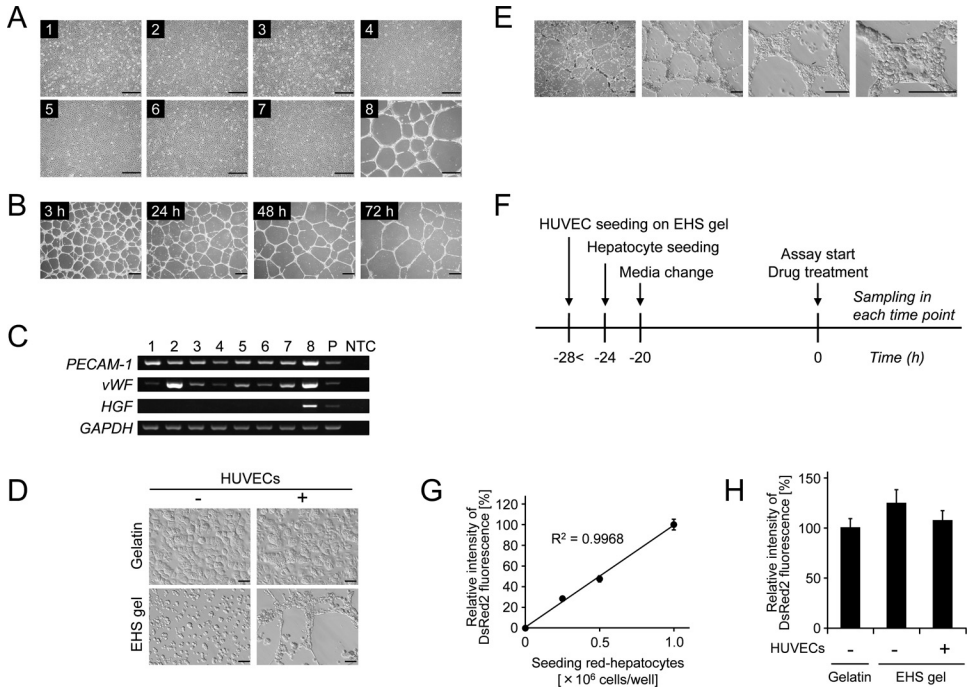

FIG. 1. Characterizations of the IVL_{EHS}. A, microscopic images of HUVECs on each scaffold material after 24 h of culture. 1, tissue-culture treated; 2, gelatin; 3, laminin; 4, fibronectin; 5, poly-D-lysine; 6, collagen type I; 7, collagen type IV; 8, growth factor-reduced EHS gel. B, time-dependent construction of the HUVEC network on EHS gel soon after seeding. C, RT-PCR analysis of HUVECs on each scaffold material: lane 1, tissue-culture treated; 2, gelatin; 3, laminin; 4, fibronectin; 5, poly-D-lysine; 6, collagen type I; 7, collagen type IV; 8, growth factor-reduced EHS gel; P, positive control (cDNA library of human adult liver); NTC, nontemplate control; glyceraldehyde-3-phosphate dehydrogenase (GAPDH), internal loading control. D and E, microscopic images of the in vitro liver tissue model consisting of primary hepatocytes and HUVEC network on EHS gel. All images were obtained 24 h after the seeding of hepatocytes. F, schemes for construction and use of IVL_{EHS}. G, the linear relationship between the signal intensity of DsRed2 fluorescence and the total amount of red hepatocytes on gelatin after 24 h of culture. H, the intensity of DsRed2 fluorescence derived from the red hepatocytes in each culture condition. Fluorescence images were obtained 24 h after the seeding of primary red hepatocytes (1.0×10^6 cells per well in 6-well plates) and then analyzed by Multi Gauge program. Data are expressed as the means ± S.E.M. Bars, 500 μm (A and B), 100 μm (D), and 200 μm (E).

Downloaded from dmd.aspetjournals.org at ASPET Journals on July 19, 2018

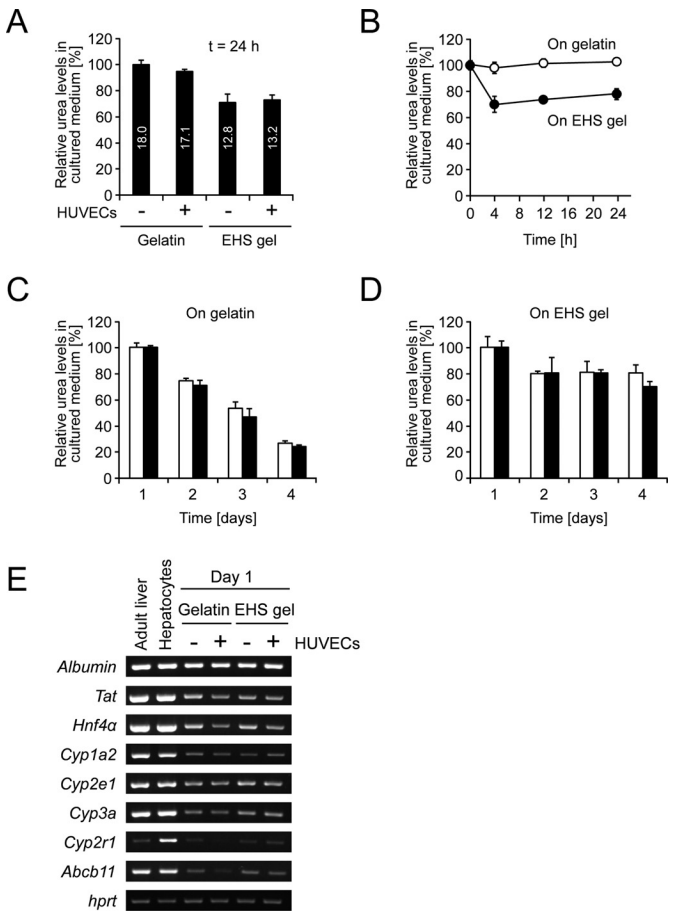

FIG. 2. Validation of hepatic function in IVL_{EHS}. A, urea levels in the culture medium in each culture condition, at 24 h. Data are calculated as ratios by referring to the urea level of hepatocyte monolayers cultured on gelatin. B, apparent decrease in urea level in culture medium incubated on EHS gel. Identical volumes of urea-containing precultured medium were incubated on gelatin or EHS gel. C and D, time-dependent change of urea productivity of hepatocyte with (closed columns) or without (open columns) HUVECs on gelatin (C) or EHS gel (D). Culture medium was changed every day over the course of the measurement period. Data are calculated as ratios by referring to the urea level on day 1 in each culture condition. Data are expressed as the means ± S.D. of triplicate determinations. E, expression levels of hepatic genes. Adult liver, mouse adult liver at 8 weeks of age; Hepatocytes, hepatocytes immediately after isolation; hprt, internal loading control.

containing precultured medium were incubated on gelatin and EHS gel. As shown in Fig. 2B, a decrease in the urea level was observed on EHS gel in the absence of primary hepatocytes, suggesting that ~30% of the urea was absorbed by the EHS gel. The urea productivity of hepatocytes was not affected by the type of scaffold material or the existence of HUVECs (Fig. 2, A and B).

To investigate whether IVL_{EHS} is superior to other models with regard to the maintenance of liver-specific functions, we examined the time-dependent change of urea productivity during the period when the HUVEC network was adequately maintained. In the case of monolayer culture on gelatin, the urea productivity of hepatocytes rapidly decreased each day (Fig. 2C). In contrast, culture on EHS gel made the cells comparatively resistant to this decrease (Fig. 2D). Although the presence of HUVECs did not enhance the potential urea productivity of hepatocytes, EHS gel was superior to gelatin with respect to the maintenance of hepatic functions.

To investigate any possible change in the hepatic gene expression, hepatocytes were cultured in each condition with or without HUVECs for 24 h and subjected to reverse transcription-polymerase chain reaction (RT-PCR) analysis. IVL_{EHS} also retained some cytochrome P450 expression at least, as well as monolayer cultured hepatocytes (Fig. 2E), suggesting that the hepatic potential of IVL_{EHS} was not lower than that of monolayer cultured hepatocytes.

Measurement of In Vitro Hepatotoxicity Induced by Acetaminophen Treatment. We next examined the hepatotoxicity in the liver tissue model induced by APAP; this treatment was intended to simulate an exogenous stimulus triggered by xenobiotic treatment. At first, to evaluate the effect of APAP on the cytotoxicity of hepatocytes, we incubated hepatocytes on gelatin with APAP at different concentrations for 36 h. Hepatocyte viability was measured by the WST-1 assay. Because 10 mM APAP was sufficient to induce hepatocyte death within 36 h (Fig. 3A), we chose 10 mM APAP as the direct toxicant concentration for the following experiments. The release of LDH into the cultured medium was measured at various time points. Differences between APAP-treated and untreated samples started to be observed 24 h after the addition of APAP (Fig. 3B). After 36-h exposure to APAP, LDH level in the culture medium of treated cells was significantly higher than in the control (Fig. 3B). Microscopic observation indicates that the monolayer-cultured hepatocytes were lethally injured, and that the normal cytoplasmic projections of spreading hepatocytes, present in control culture on gelatin, were disrupted (Fig. 3C). The hepatocytes cultured on EHS gel were also injured. The architecture of the liver tissue model, with hepatocytes massing around the HUVEC network, maintained its appearance (Fig. 3C). It is noteworthy that exposure to APAP for 36 h did not affect the final levels of LDH in any culture condition, but it did affect the time-dependent increase of LDH (Fig. 3D).

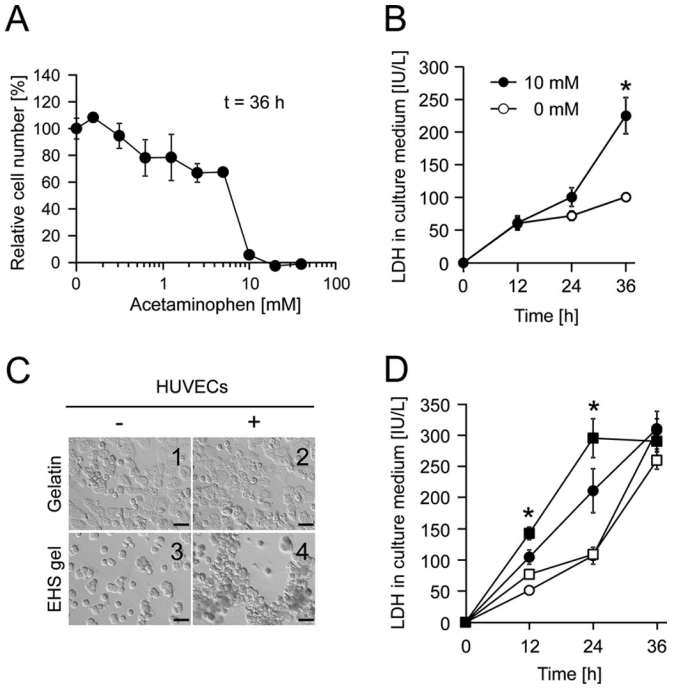

FIG. 3. Measurement of in vitro hepatotoxicity induced by acetaminophen treatment. A, dose-dependent cytotoxicity induced by APAP. Hepatocytes cultured on gelatin were treated with APAP at various concentrations for 36 h. The relative number of hepatocytes was evaluated by WST-1 assay. B, time-dependent change of LDH levels in the culture medium, for hepatocytes on gelatin with (closed circles) or without (open circles) 10 mM APAP. C, microscopic images of hepatocytes in the in vitro liver tissue model (on EHS gel with HUVEC) and other culture conditions (on gelatin with or without HUVEC, and on EHS gel without HUVEC) at 36 h after the APAP treatment. Bars, 50 μm. D, time-dependent increase of LDH in the culture medium upon 10 mM APAP treatment in each culture condition: with (squares) or without (circles) HUVEC; on gelatin (open symbols) or EHS gel (closed symbols). Data are expressed as the means ± S.D. of triplicate determinations. *, significantly different from all other groups ($P < 0.05$).

Downloaded from dmd.aspetjournals.org at ASPET Journals on July 19, 2018

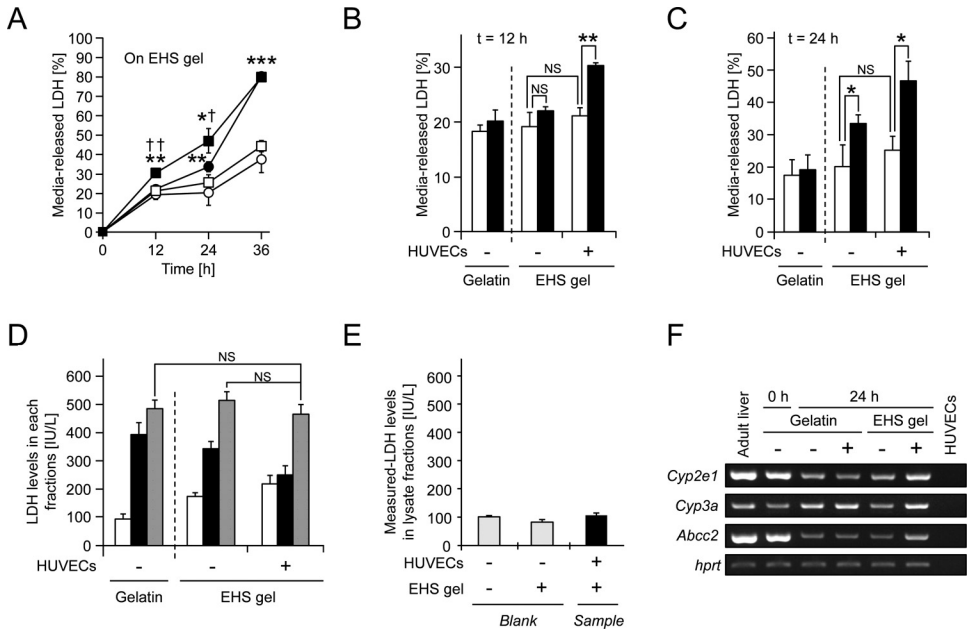

FIG. 4. The effect of construction of the in vitro liver tissue model on APAP-induced hepatotoxicity. A, time-dependent increase of LDH released by hepatocytes on EHS gel in each culture condition, with (squares) or without (circles) HUVEC and with (closed symbols) or without (open symbols) 10 mM APAP. B and C, the ratio of media-released LDH with (closed columns) or without (open columns) 10 mM APAP at 12 (B) and 24 h (C). D, LDH levels in each fraction (cultured medium, open columns; whole-cell lysate, closed columns; total, slashed columns) after 24-h incubation with 10 mM APAP in each culture condition. Data are expressed as the means ± S.D. $n = 3$–9. *, $P < 0.05$; **, $P < 0.01$; ***, $P < 0.001$, relative to the APAP-absent control; †, $P < 0.05$; ††, $P < 0.01$ relative to the HUVEC-absent control; NS, not significant. E, measured-LDH levels in HUVECs cultured on EHS gel after 24 h of culture. Blank (dot) means a non-HUVECs control. These raw data are expressed as the means ± S.D. $n = 3$. F, RT-PCR analysis of hepatocytes cultured with or without HUVECs in each condition. Adult liver, mouse adult liver at 8 weeks of age; hprt, internal loading control.

Enhancement of the Response to Acetaminophen in the IVL_{EHS}. To further investigate whether the construction of the IVL_{EHS} enhances the responsiveness of hepatocytes to APAP, we examined the media-released LDH ratio. As described in Fig. 4A, IVL_{EHS} showed an early response to acetaminophen. Twelve hours after the APAP treatment, the ratio of released LDH in the liver tissue model was already higher than in any controls (Fig. 4B). At this time point, APAP was not directly toxic to HUVECs alone. Hepatocytes alone on EHS gel were also affected by APAP-dependent toxicity after 24 h (Fig. 4C). On the other hand, at those time points, there was no significant difference in the ratio of released LDH caused by APAP treatment in hepatocytes cultured alone on gelatin (Fig. 4, B and C). Furthermore, total LDH levels in hepatocytes incubated with APAP for 24 h were not affected by the type of scaffold material (gelatin or EHS gel) or the presence of HUVECs (Fig. 4D). In this study, the existence of HUVECs had little effect on the LDH level in the culture medium (under the detectable limitation) and whole-cell lysate fraction (Fig. 4E). Under these experimental conditions, HUVECs produced far less LDH than hepatocytes; thus, the increase of LDH release in IVL_{EHS} under the APAP condition appeared to result from the rise of APAP cytotoxicity in hepatocytes. These results suggest that culture on EHS gel could prevent the depression of responsiveness in hepatocytes that is observed in monolayer culture on gelatin; the construction of the IVL_{EHS} would enhance this positive effect further. Finally, to compare the expression level of the *Cyp2e1* gene between IVL_{EHS} and other conditions, RT-PCR analysis was performed 24 h after the seeding of hepatocytes. The expression level of mouse *Cyp2e1* in IVL_{EHS} remained high, compared with other conditions (Fig. 4F). Furthermore, mercapturate, one of the APAP metabolites produced via NAPQI, was quantified by CE-TOFMS in the IVL_{EHS} and primary hepatocyte culture on EHS gel at least 12 h after the APAP treatment. As shown in Table 3, the amount of mercapturate in the IVL_{EHS} was almost the same as that in the primary hepatocyte culture.

Activities of Cytochrome P450 Isozymes in the IVL_{EHS}. The key mechanism underlying APAP hepatotoxicity is cytochrome P450-mediated NAPQI formation (David, 2005). To quantify the P450 activities as major drug-metabolizing enzyme activities in IVL_{EHS}, we quantitatively examined the amount of hydroxylated testosterones in cultured medium. Each P450 enzyme participates independently in the regioselective hydroxylation of testosterone, enabling us to simultaneously investigate the activities of multiple P450s. Testosterone was added into the IVL_{EHS} system, and its metabolites were analyzed by HPLC in their hydroxylated forms. As described in Fig. 5A, retention times of the analytes were as follows: 6β-OHT, 16.3 min; 7α-OHT, 16.9 min; 16α-OHT, 21.3 min; 16β-OHT, 23.9 min; and 2α-OHT, 26.4 min. These products (6β-OHT, 7α-OHT, 16α-OHT, 16β-OHT, and 2α-OHT) were differentially converted by specific cytochrome P450s (Cyp3a, Cyp2a4/5 and 2d9, Cyp2d9 and Cyp2b, Cyp2c29 and Cyp2e, and Cyp2d), respectively. The metabolite profile indicates that activities of P450 isozymes in IVL_{EHS} were higher than those under other conditions (Fig. 5B).

Discussion

Positive Effect of the Construction of IVL_{EHS}. In this study, we showed that culture of hepatocytes in a model that resembles the structure of hepatic tissue is superior to monolayer culture of primary hepatocytes, both in regard to the maintenance of some hepatic genes and the response to xenobiotics, at least in the case of APAP. These findings suggest that this system could be applied to the evaluation of compound-associated hepatotoxicity. Because primary hepatocytes have a more complete set of phase I- and II-metabolizing enzymes than immortalized cell lines, they have been used to develop assay systems that are more representative of in vivo hepatocytes (Dambach et al., 2005). A monolayer system consisting of confluent culture of

TABLE 3

Concentration of 3-(N-acetyl-L-cysteine-S-yl)acetaminophen, mercapturate, in each cellular extraction detected by CE-TOFMS analysis

Data are expressed as the means ± S.D. $n = 3$. There is no significant difference between APAP-treated samples.

HUVEC	APAP Treatment	Mercapturate
		μM/ml extraction
–	–	N.D.
–	+	0.22 ± 0.0414
+	–	N.D.
+	+	0.19 ± 0.0052

N.D., not detected.

Downloaded from dmd.aspetjournals.org at ASPET Journals on July 19, 2018

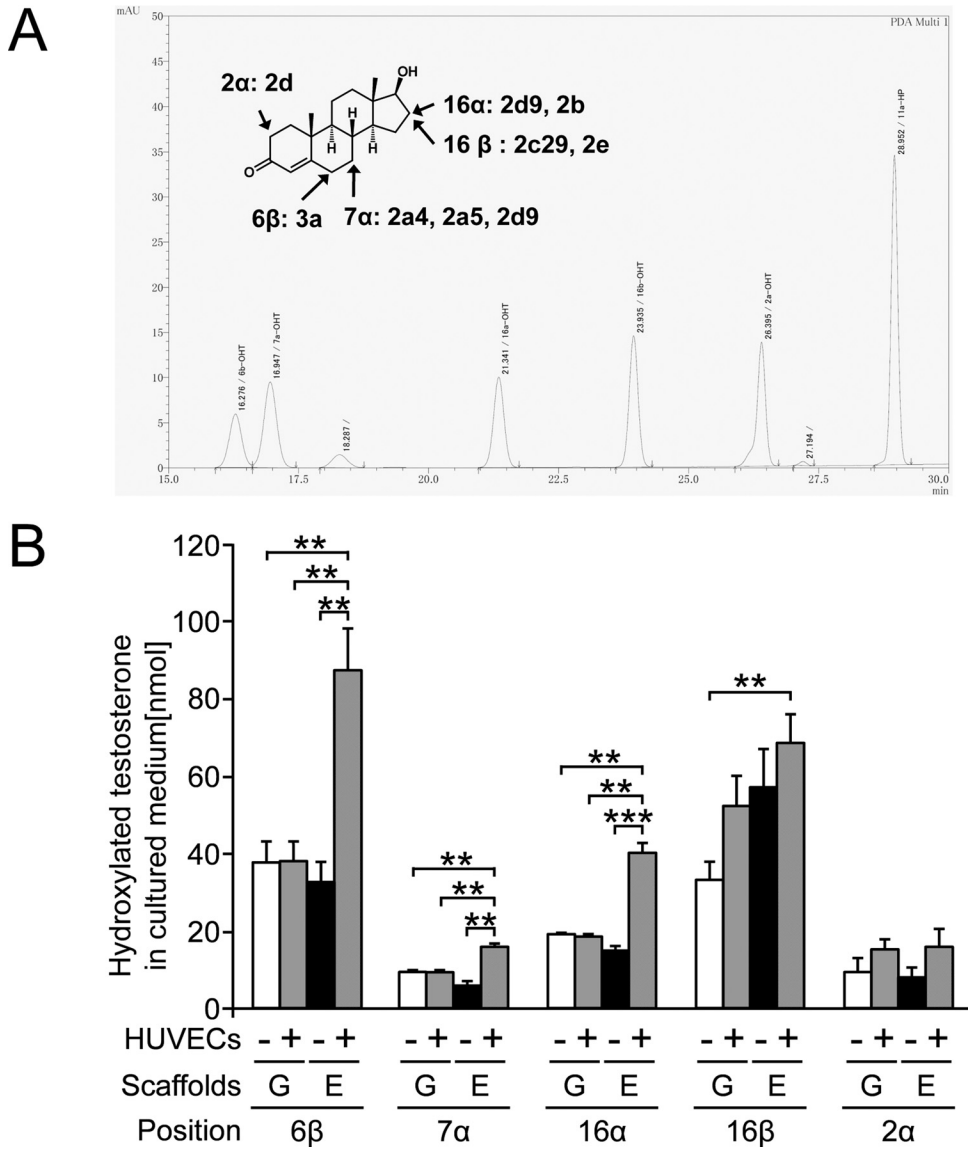

FIG. 5. Testosterone hydroxylation in IVL_{EHS} system. A, HPLC chromatograms of each standard; 6β-OHT (16.3 min), 7α-OHT (16.9 min), 16α-OHT (21.3 min), 16β-OHT (23.9 min), 2α-OHT (26.4 min), and 11α-HP (29 min, as an internal control). B, the amount of each hydroxylated testosterones in culture medium. Data are expressed as the means ± S.D. of triplicate determinations. G, gelatin; E, EHS gel. **, $P < 0.01$; ***, $P < 0.001$.

freshly isolated hepatocytes is already a well established model that provides a better assessment of the metabolic effects and potential hepatotoxicity of interesting compounds (Kikkawa et al., 2006; Hewitt et al., 2007). However, this widely used model has some limitations: low proliferative capacity (not exceeding a few days), loss of liver-specific functions such as drug-metabolizing enzymes, and others. These phenotypic changes reportedly occur early during the isolation process and after seeding, probably as a result of their adaptation to microenvironmental alterations (Guillouzo, 1998). Therefore, we aimed to construct a sophisticated culture condition that mimics the situation in the liver, and examine its utility.

We succeeded in developing a structure that resembles hepatic tissue on EHS gel (Fig. 1). It is well known that the EHS gel induces rapid formation of a capillary-like tubular network of endothelial cells and can preserve hepatocyte functions such as albumin production, expression of some hepatic genes, and others. (Bissell et al., 1987; Kubota et al., 1988). Because EHS gel is an extract of basement membrane proteins derived from the EHS tumor, it consists of various components such as laminin, collagen type IV, proteases such as matrix metallopeptidases, growth factors, and other proteins (Kleinman and Martin, 2005); therefore, in this study, we used growth factor reduced EHS gel to reduce the number of factors that could influence cellular phenotypes. In our examinations, no scaffold material other than EHS gel allowed HUVECs to form networks and generate three-dimensional structures. Further study demonstrated that this cocultivation system of hepatocytes and endothelial cell network was characterized by the expression of HGF, with the HUVEC network functioning as a HGF donor. HGF plays a key role in liver development and maintenance (Schmidt et al., 1995; Matsumoto et al., 2001). Because the active migration of hepatocytes and subsequent adhesion occurred only in the presence of a HUVEC network structure, this phenomenon must be mediated by HGF from HUVEC network. In support of this idea, our research group also found that high levels of soluble HGF protein inhibited hepatocyte migration (Y. Tagawa and S. Kobayashi, unpublished observation). These observations are in agreement with previous reports (Nahmias et al., 2006; Soto-Gutierrez et al., 2010).

Indeed, various factors are able to affect cellular functions of hepatocytes in vitro, and these factors are usually classified into 3 groups, as follows: 1) soluble factors such as cytokines; 2) ECM components that regulate cell behaviors via cell adhesion processes; and 3) cell-cell interactions (Guillouzo et al., 1993). Heterotypic

Downloaded from dmd.aspetjournals.org at ASPET Journals on July 19, 2018

cell-cell interactions between parenchymal cells and nonparenchymal neighbors play an especially important role in the preservation and modulation of hepatocyte phenotypes in vitro as well as in vivo (Bhatia et al., 1999). As we described under *Results*, the hepatocytes in our in vitro liver tissue model were able to benefit from all three groups of factors: HGF, EHS gel, and hepatocyte-HUVEC interactions correspond to cytokines, ECM, and heterotypic interactions, respectively. Although the specific molecular mechanisms involved in the hepatocyte recruitment process needs to be elucidated, our results suggest the importance of the nonparenchymal cell population for the ex vivo recapitulation of the in vivo liver environment. Further study will shed light on these molecular mechanism(s) and the development of more suitable biomaterials for the construction of in vitro liver tissue models.

Application of IVL_{EHS} to Hepatotoxicity Studies. At present, accumulating evidence suggests that the presence of nonparenchymal cells would be able to support parenchymal cells in vitro as they do in vivo. Nahmias et al. (2006) have reported the endothelium-mediated recruitment of hepatocytes on EHS gel, as well as the stabilization of hepatic function, such as the expression and activity of some *Cyp* genes, in hepatic tissue models that were stable in long-term culture (Soto-Gutierrez et al., 2010). Their experimental evidence supports the future applicability of liver tissue models to the development of bioartificial liver systems. However, their studies were limited to the EHS gel culture and did not include comparison to the gold-standard model. Therefore, we focused on the differences in hepatic functions between our liver tissue model and monolayer culture of hepatocytes.

As shown in Fig. 2, the initial capability of hepatocytes to produce urea depends very little on the culture conditions. However, culture on EHS gel more efficiently preserved hepatic function than culture on gelatin. Under conditions of low external stress, the positive effect of EHS gel is so large that it is difficult to determine the exact contribution of cocultivation with endothelial cells, at least in short-term culture. On the other hand, the construction of a structure resembling hepatic tissue reinforced the responsiveness of hepatocytes to acetaminophen treatment (Figs. 3 and 4).

Acetaminophen is a commonly used analgesic/antipyretic drug, and its overdose induces liver injury in humans and experimental animals. This model hepatotoxicant is converted by a cytochrome P450 enzyme into its reactive metabolite form, NAPQI. In particular, CYP2E1, -1A2, -3A4, and -2A6 play major roles in this oxidation process (James et al., 2003). At therapeutic doses of acetaminophen, the reactive metabolite is efficiently detoxified by glutathione conjugation. However, at a toxic dose, glutathione is depleted by this conjugation, and the excess metabolite covalently binds to protein, resulting in the induction of oxidative stress and the development of toxicity (Jaeschke et al., 2003; James et al., 2003; Reid et al., 2005).

According to in vivo experiments and clinical evidence, these events occur within a few hours after the administration of a toxic dose of acetaminophen. Furthermore, previous studies have indicated that the response of parenchymal cells to acetaminophen might be amplified by contributions from nonparenchymal cells such as liver sinusoidal endothelial cells and Kupffer cells (DeLeve et al., 1997; Ito et al., 2003; Holt et al., 2010). However, the toxicity observed in vitro monolayer culture models occurs much later than in vivo toxicity. With regard to these concerns, the liver tissue model includes several improvements that better mimic the in vivo situation. In fact, our results suggest that the response of hepatocytes to APAP toxicity was reinforced in IVL_{EHS}, probably via the maintenance of expression or up-regulation of cytochromes such as Cyp2e1. It is noteworthy that the activities of drug-metabolizing enzymes were higher in IVL_{EHS} than under other conditions (Fig. 5).

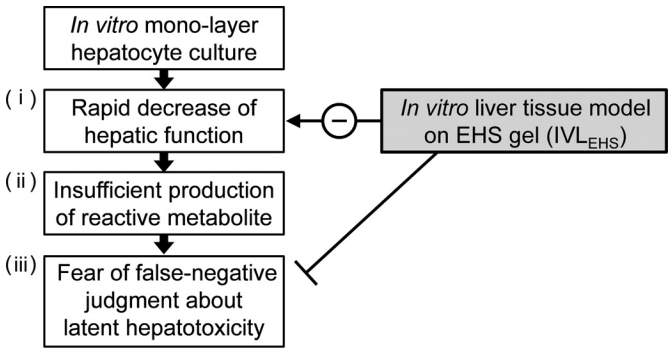

FIG. 6. Schematic illustration of the beneficial effect of IVL_{EHS} construction on both the responsiveness of hepatocytes and evaluation of hepatotoxicity.

So far, there have been no reports of the direct detection of NAPQI in hepatocytes, particularly in hepatocytes cultured on EHS gel. However, in this study, to confirm the functional metabolism of APAP in IVL_{EHS}, its cellular extract was assayed for mercapturate by CE-TOFMS (Table 3). This mercapturate form is produced metabolically from APAP via NAPQI (Soga et al., 2006). Because the NAPQI-dependent cytotoxicity is caused after the saturation of detoxification capability, intracellular administration of mercapturate suggests that IVL_{EHS} maintains a higher (or at least equivalent) metabolizing capacity than monocultures on EHS gel.

Conclusions

In summary, this study revealed the superiority of liver tissue models over the monolayer culture of hepatocytes. In short-term culture, EHS gel effectively maintained hepatic function; the further introduction of endothelial cells contributed to an early response to hepatotoxicant that mirrors the kinetics of the response in vivo. These results suggest that IVL_{EHS} is suitable for use as a compound-associated hepatotoxicity system and is superior to existing in vitro monolayer systems (Fig. 6). It is noteworthy that we performed the minimum modification necessary to archive the hepatic tissue-like structure. Many ingenious attempts have been made to mimic the in vivo liver architecture and developed improved systems for evaluating hepatotoxicity, e.g., micropatterning (El-Ali et al., 2006; Khetani and Bhatia, 2008), shear stress (Vinci et al., 2011), P450-inducers such as phenobarbital, and others. Incorporation of these technologies will contribute to the further improvement of our strategy.

Acknowledgments

We thank all members of our laboratory for their excellent animal care.

Authorship Contributions

Participated in research design: Toyoda and Tagawa.

Conducted experiments: Toyoda, Tamai, Kobayashi, Soga, and Tagawa.

Contributed new reagents or analytic tools: Kobayashi, Fujiyama, Soga, and Tagawa.

Performed data analysis: Toyoda, Tamai, and Kashikura.

Wrote or contributed to the writing of the manuscript: Toyoda and Tagawa.

References

Bhatia SN, Balis UJ, Yarmush ML, and Toner M (1998) Microfabrication of hepatocyte/fibroblast co-cultures: role of homotypic cell interactions. *Biotechnol Prog* **14:**378–387.

Bhatia SN, Balis UJ, Yarmush ML, and Toner M (1999) Effect of cell-cell interactions in preservation of cellular phenotype: cocultivation of hepatocytes and nonparenchymal cells. *FASEB J* **13:**1883–1900.

Bissell DM, Arenson DM, Maher JJ, and Roll FJ (1987) Support of cultured hepatocytes by a laminin-rich gel. Evidence for a functionally significant subendothelial matrix in normal rat liver. *J Clin Invest* **79:**801–812.

Dambach DM, Andrews BA, and Moulin F (2005) New technologies and screening strategies for hepatotoxicity: use of in vitro models. *Toxicol Pathol* **33:**17–26.

Downloaded from dmd.aspetjournals.org at ASPET Journals on July 19, 2018

David JP (2005) The molecular toxicology of acetaminophen. *Drug Metab Rev* **37:**581–594.
DeLeve LD, Wang X, Kaplowitz N, Shulman HM, Bart JA, and van der Hoek A (1997) Sinusoidal endothelial cells as a target for acetaminophen toxicity. Direct action versus requirement for hepatocyte activation in different mouse strains. *Biochem Pharmacol* **53:** 1339–1345.
El-Ali J, Sorger PK, and Jensen KF (2006) Cells on chips. *Nature* **442:**403–411.
Gleeson MP, Hersey A, Montanari D, and Overington J (2011) Probing the links between in vitro potency, ADMET and physicochemical parameters. *Nat Rev Drug Discov* **10:**197–208.
Guillouzo A (1998) Liver cell models in in vitro toxicology. *Environ Health Perspect* **106 (Suppl 2):**511–532.
Guillouzo A, Morel F, Fardel O, and Meunier B (1993) Use of human hepatocyte cultures for drug metabolism studies. *Toxicology* **82:**209–219.
Hayes MA and Pickering DB (1985) Comparative cytopathology of primary rat hepatocyte cultures exposed to aflatoxin B1, acetaminophen, and other hepatotoxins. *Toxicol Appl Pharmacol* **80:**345–356.
Hewitt NJ, Lechón MJ, Houston JB, Hallifax D, Brown HS, Maurel P, Kenna JG, Gustavsson L, Lohmann C, Skonberg C, et al. (2007) Primary hepatocytes: current understanding of the regulation of metabolic enzymes and transporter proteins, and pharmaceutical practice for the use of hepatocytes in metabolism, enzyme induction, transporter, clearance, and hepatotoxicity studies. *Drug Metab Rev* **39:**159–234.
Holt MP, Yin H, and Ju C (2010) Exacerbation of acetaminophen-induced disturbances of liver sinusoidal endothelial cells in the absence of Kupffer cells in mice. *Toxicol Lett* **194:**34–41.
Ito Y, Bethea NW, Abril ER, and McCuskey RS (2003) Early hepatic microvascular injury in response to acetaminophen toxicity. *Microcirculation* **10:**391–400.
Jaeschke H, Gores GJ, Cederbaum AI, Hinson JA, Pessayre D, and Lemasters JJ (2002) Mechanisms of hepatotoxicity. *Toxicol Sci* **65:**166–176.
Jaeschke H, Knight TR, and Bajt ML (2003) The role of oxidant stress and reactive nitrogen species in acetaminophen hepatotoxicity. *Toxicol Lett* **144:**279–288.
James LP, Mayeux PR, and Hinson JA (2003) Acetaminophen-induced hepatotoxicity. *Drug Metab Dispos* **31:**1499–1506.
Kaplowitz N (2005) Idiosyncratic drug hepatotoxicity. *Nat Rev Drug Discov* **4:**489–499.
Khetani SR and Bhatia SN (2008) Microscale culture of human liver cells for drug development. *Nat Biotechnol* **26:**120–126.
Kidambi S, Yarmush RS, Novik E, Chao P, Yarmush ML, and Nahmias Y (2009) Oxygen-mediated enhancement of primary hepatocyte metabolism, functional polarization, gene expression, and drug clearance. *Proc Natl Acad Sci USA* **106:**15714–15719.
Kikkawa R, Fujikawa M, Yamamoto T, Hamada Y, Yamada H, and Horii I (2006) In vivo hepatotoxicity study of rats in comparison with in vitro hepatotoxicity screening system. *J Toxicol Sci* **31:**23–34.
Kleinman HK and Martin GR (2005) Matrigel: basement membrane matrix with biological activity. *Semin Cancer Biol* **15:**378–386.
Kleinman HK, Philp D, and Hoffman MP (2003) Role of the extracellular matrix in morphogenesis. *Curr Opin Biotechnol* **14:**526–532.
Kola I and Landis J (2004) Can the pharmaceutical industry reduce attrition rates? *Nat Rev Drug Discov* **3:**711–715.
Kubota Y, Kleinman HK, Martin GR, and Lawley TJ (1988) Role of laminin and basement membrane in the morphological differentiation of human endothelial cells into capillary-like structures. *J Cell Biol* **107:**1589–1598.
Kwong E, Higgins J, and Templeton AC (2011) Strategies for bringing drug delivery tools into discovery. *Int J Pharm* **412:**1–7.
Lee SS, Buters JT, Pineau T, Fernandez-Salguero P, and Gonzalez FJ (1996) Role of CYP2E1 in the hepatotoxicity of acetaminophen. *J Biol Chem* **271:**12063–12067.
Matsumoto K, Yoshitomi H, Rossant J, and Zaret KS (2001) Liver organogenesis promoted by endothelial cells prior to vascular function. *Science* **294:**559–563.
Nahmias Y, Schwartz RE, Hu WS, Verfaillie CM, and Odde DJ (2006) Endothelium-mediated hepatocyte recruitment in the establishment of liver-like tissue in vitro. *Tissue Eng* **12:**1627–1638.
Ogawa S, Tagawa Y, Kamiyoshi A, Suzuki A, Nakayama J, Hashikura Y, and Miyagawa S (2005) Crucial roles of mesodermal cell lineages in a murine embryonic stem cell-derived in vitro liver organogenesis system. *Stem Cells* **23:**903–913.
Paul SM, Mytelka DS, Dunwiddie CT, Persinger CC, Munos BH, Lindborg SR, and Schacht AL (2010) How to improve R&D productivity: the pharmaceutical industry's grand challenge. *Nat Rev Drug Discov* **9:**203–214.
Reid AB, Kurten RC, McCullough SS, Brock RW, and Hinson JA (2005) Mechanisms of acetaminophen-induced hepatotoxicity: role of oxidative stress and mitochondrial permeability transition in freshly isolated mouse hepatocytes. *J Pharmacol Exp Ther* **312:**509–516.
Schmidt C, Bladt F, Goedecke S, Brinkmann V, Zschiesche W, Sharpe M, Gherardi E, and Birchmeier C (1995) Scatter factor/hepatocyte growth factor is essential for liver development. *Nature* **373:**699–702.
Seglen PO (1976) Preparation of isolated rat liver cells. *Methods Cell Biol* **13:**29–83.
Soga T, Baran R, Suematsu M, Ueno Y, Ikeda S, Sakurakawa T, Kakazu Y, Ishikawa T, Robert M, Nishioka T, et al. (2006) Differential metabolomics reveals ophthalmic acid as an oxidative stress biomarker indicating hepatic glutathione consumption. *J Biol Chem* **281:**16768–16776.
Soga T, Igarashi K, Ito C, Mizobuchi K, Zimmermann HP, and Tomita M (2009) Metabolomic profiling of anionic metabolites by capillary electrophoresis mass spectrometry. *Anal Chem* **81:**6165–6174.
Soto-Gutierrez A, Navarro-Alvarez N, Yagi H, Nahmias Y, Yarmush ML, and Kobayashi N (2010) Engineering of an hepatic organoid to develop liver assist devices. *Cell Transplant* **19:**815–822.
Strain AJ (1999) Ex vivo liver cell morphogenesis: one step nearer to the bioartificial liver? *Hepatology* **29:**288–290.
Takashi H, Katsumi M, and Toshihiro A (2007) Hepatocytes maintain their function on basement membrane formed by epithelial cells. *Biochem Biophys Res Commun* **359:**151–156.
Tsutsui M, Ogawa S, Inada Y, Tomioka E, Kamiyoshi A, Tanaka S, Kishida T, Nishiyama M, Murakami M, Kuroda J, et al. (2006) Characterization of cytochrome P450 expression in murine embryonic stem cell-derived hepatic tissue system. *Drug Metab Dispos* **34:**696–701.
Vinci B, Duret C, Klieber S, Gerbal-Chaloin S, Sa-Cunha A, Laporte S, Suc B, Maurel P, Ahluwalia A, and Daujat-Chavanieu M (2011) Modular bioreactor for primary human hepatocyte culture: medium flow stimulates expression and activity of detoxification genes. *Biotechnol J* **6:**554–564.

Address correspondence to: Yoh-ichi Tagawa, Associate Professor, Department of Biomolecular Engineering, Graduate School of Bioscience and Biotechnology, Tokyo Institute of Technology, 4259-B-51 Nagatsuta-cho, Midori-ku, Yokohama 226-8501, Japan. E-mail: ytagawa@bio.titech.ac.jp

Downloaded from dmd.aspetjournals.org at ASPET Journals on July 19, 2018